Vibrations of the Phenoxyl Radical

Jens Spanget-Larsen,[†,‡,§] Michał Gil,[†,‡,||] Alexandr Gorski,[†,‡,||] Daniel M. Blake,[†] Jacek Waluk,[†,‡,||] and J. George Radziszewski*[,†,‡]

Contribution from the National Renewable Energy Laboratory (NREL), 1617 Cole Boulevard, Golden, Colorado 80401, Department of Chemical Engineering, Colorado School of Mines, Golden, Colorado 80401, Department of Chemistry, Roskilde University (RUC), DK-4000 Roskilde, Denmark, and the Institute of Physical Chemistry, Polish Academy of Sciences, Kasprzaka 44, 01-224 Warsaw, Poland

Received June 4, 2001

Abstract: Phenoxyl radical (C_6H_5O) was prepared photochemically in low-temperature argon matrices. The infrared absorption spectra were obtained for C_6H_5O and for the isotopically labeled species C_6D_5O and 1-$^{13}C^{12}C_5H_5O$. All but one IR-active fundamental vibrations were detected, most of them not previously observed. Combination of results from IR linear dichroism measurements on photooriented samples, determination of absolute IR intensities with the help of internal standards, analysis of isotopic shifts, and quantum chemical predictions (B3LYP/cc-pVTZ) led to a detailed assignment of phenoxyl radical vibrations. Significant frequency shifts are observed with respect to previously reported data based on resonance Raman studies in polar solutions. For some vibrations, these shifts reflect environment-induced structural changes, such as increase of the quinoid character of the phenoxyl radical in polar media. In particular, the frequency of the CO stretching vibration, readily observable in both IR and Raman experiments, is extremely sensitive to the environment and can thus be used to probe its polarity.

1. Introduction

Because of its major role as a transient species in a wide range of environmental and biological processes, the structure and chemistry of the phenoxyl radical (C_6H_5O, **1**) is a subject of continuous interest. It is one of the key intermediates in the combustion of aromatic compounds.[1−4] By itself, or more often in metal-complexed and substituted forms, the phenoxyl radical takes part in biocatalysis,[5−7] protein redox reactions,[8−10] electron-transfer reactions involving carotenoids,[11,12] lignin biosynthesis,[13−15] phenol-inhibited oxidation of hydrocarbons,[16] and green plant photosynthesis.[17]

The identity of this radical has been well established in electron-spin resonance (ESR) and ENDOR studies.[18−31] Numerous works have investigated the pathways of thermal decomposition of **1** and probed its reactivity, in particular toward oxygen and nitrogen oxides.[4,32−47] These studies often require time-resolved spectroscopic measurements in the regions of the electronic transitions of **1**. Electronic absorption spectra of the phenoxyl radical have been obtained both in gas and condensed phases[4,40,48−58] and discussed in a number of theoretical papers.[43,59−63]

† National Renewable Energy Laboratory.
‡ Colorado School of Mines.
§ Roskilde University.
|| Polish Academy of Sciences.

(1) Haynes, D. S. In *Fossil Fuel Combustion*; Wiley-Interscience: New York, 1991, p 261.
(2) Bockhorn, H. *Soot Formation in Combustion*; Springer-Verlag: New York, 1993.
(3) Vovelle, C.; Delfau, J. L. *NATO Sci. Ser., Ser. C* **2000**, 547.
(4) Platz, J.; Nielsen, O. J.; Wallington, T. J.; Ball, J. C.; Hurley, M. D.; Straccia, A. M.; Schneider, W. F.; Sehested, J. *J. Phys. Chem. A* **1998**, *102*, 7964.
(5) Casella, L.; De Gioia, L.; Silvestri, G. F.; Monzani, E.; Redaelli, C.; Roncone, R.; Santagostini, L. *J. Inorg. Biochem.* **2000**, *79*, 31.
(6) Shimazaki, Y.; Huth, S.; Odani, A.; Yamauchi, O. *Angew. Chem., Int. Ed.* **2000**, *39*, 1666.
(7) Itoh, S.; Taki, M.; Fukuzumi, S. *Coord. Chem. Rev.* **2000**, *198*, 3.
(8) Irwin, J. A.; Ostdal, H.; Davies, M. J. *Arch. Biochem. Biophys.* **1999**, *362*, 94.
(9) Kagan, V. E.; Tyurina, Y. Y. *Ann. N.Y. Acad. Sci.* **1998**, 854.
(10) Eriksson, L. E.; Hyde, J. S.; Ehrenberg, A. *Biochim. Biophys. Acta* **1969**, *192*, 211.
(11) Mortensen, A.; Everett, S. A.; Skibsted, L. H. *Phytochem. Phytopharm.* **2000**, 185.
(12) Mortensen, A.; Skibsted, L. H. *Free Radical Res.* **1996**, *25*, 515.
(13) Davin, L. B.; Wang, H.-B.; Crowell, A. L.; Bedgar, D. L.; Martin, D. M.; Sarkanen, S.; Lewis, N. G. *Science (Washington, D.C.)* **1997**, *275*, 362.
(14) Lewis, N. G.; Davin, L. B. *ACS Symp. Ser.* **1998**, *697*, 334.
(15) Sarkanen, S. *ACS Symp. Ser.* **1998**, *697*, 194.
(16) Fujii, N.; Asaba, T. *Proceeedings of the 14th Symposium on Combustion*; The Combustion Institute: Pittsburgh, PA, 1973, p 433.
(17) Weaver, E. C. *Annu. Rev. Plant. Physiol.* **1968**, *19*, 283.
(18) Stone, T. J.; Waters, W. A. *Proc. Chem. Soc., London* **1962**, 253.
(19) Stone, T. J.; Waters, W. A. *J. Chem. Soc.* **1964**, 213.
(20) Dixon, W. T.; Norman, R. O. C. *Proc. Chem. Soc., London* **1963**, 97.
(21) Dixon, W. T.; Norman, R. O. C. *J. Chem. Soc.* **1964**, 4857.
(22) Neta, P.; Fessenden, R. W. *J. Phys. Chem.* **1974**, *78*, 523.
(23) Dixon, W. T.; Murphy, D. *J. Chem. Soc., Faraday Trans. 2* **1976**, *72*, 1221.
(24) Dewar, M. J. S.; David, D. E. *J. Am. Chem. Soc.* **1980**, *102*, 7387.
(25) Tripathi, G. N. R.; Sun, Q.; Armstrong, D. A.; Chipman, D. M.; Schuler, R. H. *J. Phys. Chem.* **1992**, *96*, 5344.
(26) Hurum, D. C.; Kreilick, R. W. *J. Phys. Chem.* **1995**, *99*, 11813.
(27) Pople, J. A.; Beveridge, D. L.; Dobosh, P. A. *J. Am. Chem. Soc.* **1968**, *90*, 4021.
(28) Lloyd, R. V.; Wood, D. E. *J. Am. Chem. Soc.* **1974**, *96*, 659.
(29) Hinchliffe, A. *Chem. Phys. Lett.* **1974**, *27*, 454.
(30) Shinagawa, Y.; Shinagawa, Y. *J. Am. Chem. Soc.* **1978**, *100*, 67.
(31) Armstrong, D. R.; Cameron, C.; Nonhebel, D.; Perkins, P. G. *J. Chem. Soc., Perkin Trans. 2* **1983**, 569.
(32) Frank, P.; Herzler, J.; Just, T.; Wahl, C. *Proceedings of the 25th International Symposium on Combustion*; The Combustion Institute: Pittsburgh, PA, 1994, p 833.
(33) Lin, C.-Y.; Lin, M. C. *Int. J. Chem. Kinet.* **1985**, *17*, 1025; *J. Phys. Chem.* **1986**, *90*, 425.
(34) Yu, T.; Mebel, A. M.; Lin, M. C. *J. Phys. Org. Chem.* **1995**, *8*, 47.

10.1021/ja0113596 CCC: $20.00
Published on Web 10/23/2001

Vibrational spectroscopy studies of **1** and its derivatives have almost exclusively been based on resonance Raman (RR) measurements.[64−81] These have led to controversies not only with respect to the assignment of the strongest Raman band[73,83−84] but also concerning the identity of the observed species.[75,76] The results obtained in various laboratories have provided a total of 10 bands that were assigned to the vibrations of **1**. Given that the number of Raman active fundamental vibrations is 30, most of the fundamentals of **1** thus remain unknown. The situation regarding IR studies is much worse. No systematic investigations of **1** have been undertaken so far. Only the values for the strongest IR band in several isotopomers of **1** have been reported, in connection with probing the structure of tyrosine radicals, present in many metalloenzymes.[82]

Theoretical prediction of the molecular and vibrational structure of **1** is not straightforward and has led to diverging conclusions regarding IR band assignments.[83,85] Many calculations predict an inadequate molecular geometry of **1** and thus fail to reproduce the observed vibrational pattern.[83−89] In particular, the optimized values of the C−O distance vary between those of typical single and double bonds, spanning a range of 1.22−1.38 Å.[83]

Resonance Raman and IR studies of **1** and its derivatives have been performed in vivo or in a strongly interacting environment. These studies often involve ion complexes of the radical. Hence, the spectral features of **1** tend to be significantly perturbed by interactions with counterpartners and with the environment. Some of the phenoxyl radical vibrations seem to be sensitive probes of such interactions.[88] In the absence of reference data for the unperturbed radical, spectroscopic assignments are of somewhat limited use, and tuning up the theoretical approach is also hindered. No cold gas phase (supersonic jet expansion) or ground-state matrix isolation data have been reported so far.

In this work, we present the results of photochemistry and IR spectroscopy studies of matrix-isolated phenoxyl radical. The weak interactions of the guest radicals with the noble gas host matrices make a direct comparison with theoretical predictions for the isolated radical legitimate. A low-temperature matrix provides a rotation-free environment and therefore facilitates photoorientation and linear dichroism measurements,[91] which ultimately may lead to assignment of observed transition symmetries. Use of internal intensity standards allows for determination of absolute intensities, thus making vibrational characterization of phenoxyl radical much more complete. Our assignments for **1** are confirmed and reinforced by comparison with the data obtained for isotopically substituted C_6D_5O (**2**) and 1-$^{13}C^{12}C_5H_5O$ (**3**) samples and with the results of B3LYP/cc-pVTZ calculations.

The present study of the phenoxyl radical is part of a series which also includes spectral investigations of phenyl,[92−94] phenyl peroxy, phenyl vinyl, and cyclopentadienyl radicals. These

(35) Colussi, A. J.; Zabel, F.; Benson, S. W. *Int. J. Chem. Kinet.* **1977**, *9*, 161.
(36) Harrison, A. G.; Honnen, L. R.; Dauben, H. J.; Lossing, F. P. *J. Am. Chem. Soc.* **1960**, *82*, 5593.
(37) Schmoltner, A.-M.; Anex, D. S.; Lee, Y. T. *J. Phys. Chem.* **1991**, *96*, 1236.
(38) Olivella, S.; Sole, A.; Garcia-Raso, A. *J. Phys. Chem.* **1995**, *99*, 10549.
(39) Berho, F.; Caralp, F.; Rayez, M.-T.; Lesclaux, R.; Ratajczak, E. *J. Phys. Chem. A* **1998**, *102*, 1.
(40) Tao, Z.; Li, Z. *Int. J. Chem. Kinet.* **1999**, *31*, 65.
(41) Berho, F.; Lesclaux, R. *Chem. Phys. Lett.* **1997**, *279*, 289.
(42) Denisov, E. T.; Drozdova, T. I. *Kinet. Catal. (Transl. of Kinet. Katal.)* **1997**, *38*, 35.
(43) Liu, R.; Morokuma, K.; Mebel, A. M.; Lin, M. C. *J. Phys. Chem.* **1996**, *100*, 9314.
(44) Buth, R.; Hoyerman, K.; Seeba, J. *Proceedings of the 25th International Symposium on Combustion*; The Combustion Institute: Pittsburgh, PA, 1994, p 841.
(45) He, Y. Z.; Mallard, W. G.; Tsang, J. *J. Phys. Chem.* **1992**, *92*, 2201.
(46) Mulcahy, M. F. R.; Williams, D. J. *Nature (London)* **1963**, *199*, 761.
(47) Mulcahy, M. F. R.; Williams, D. J. *Aust. J. Chem.* **1965**, *18*, 20.
(48) Land, E. J.; Porter, G.; Strachan, E. *Trans. Faraday Soc.* **1961**, *57*, 1885.
(49) Porter, G.; Strachan, E. *Trans. Faraday Soc.* **1958**, *54*, 1595.
(50) Roebber, J. L. *J. Chem. Phys.* **1962**, *37*, 1974.
(51) Ward, B. *Spectrochim. Acta, Part A* **1968**, *24*, 813.
(52) Bent, D. V.; Hayon, E. *J. Am. Chem. Soc.* **1975**, *97*, 2599.
(53) Schuler, R. H.; Buzzard, G. K. *Int. J. Radiat. Phys. Chem.* **1976**, *8*, 563.
(54) Johnston, L. J.; Mathivanan, N.; Negri, F.; Siebrand, W.; Zerbetto, F. *Can. J. Chem.* **1993**, *71*, 1655.
(55) Pullin, D.; Andrews, L. *THEOCHEM* **1982**, *95*, 181.
(56) Kajii, Y.; Obi, K.; Nakashima, N.; Yoshihara, K. *J. Chem. Phys.* **1984**, *87*, 5059.
(57) Gunion, R. M.; Gilles, M.; Polak, M.; Lineberger, W. C. *Int. J. Mass Spectrom. Ion. Processes* **1992**, *117*, 621.
(58) Sato, S.; Mikami, N. *J. Phys. Chem.* **1996**, *100*, 4765.
(59) Hinchliffe, A.; Steinbank, R. E.; Ali, M. A. *Theor. Chim. Acta* **1966**, *5*, 95.
(60) Chang, H. M.; Jaffe, H. H. *Chem. Phys. Lett.* **1973**, *23*, 146.
(61) Chang, H. M.; Jaffe, H. H.; Masmandis, C. A. *J. Phys. Chem.* **1975**, *79*, 1118.
(62) Takahashi, J.; Shida, T. *Bull. Chem. Soc. Jpn.* **1994**, *67*, 2038.
(63) Takahashi, J.; Momose, T.; Shida, T. *Bull. Chem. Soc. Jpn.* **1994**, *67*, 964.
(64) Beck, S. M.; Brus, L. E. *J. Chem. Phys.* **1982**, *76*, 4700.
(65) Tripathi, G. N. R.; Schuler, R. M. *Chem. Phys. Lett.* **1983**, *98*, 594.
(66) Tripathi, G. N. R.; Schuler, R. M. *J. Chem. Phys.* **1984**, *81*, 113.
(67) Tripathi, G. N. R.; Schuler, R. M. *J. Phys. Chem.* **1988**, *92*, 5129.
(68) Tripathi, G. N. R In *Time-Resolved Spectroscopy*; Clark, R. J. H., Hester, R. E., Eds.; Wiley: New York, 1989, p 157.
(69) Tripathi, G. N. R. *J. Phys. Chem. A* **1998**, *102*, 2388.
(70) Tripathi, G. N. R.; Schuler, R. M. *J. Chem. Soc., Faraday Trans.* **1993**, *89*, 4177.
(71) Johnson, C. R.; Ludwig, M.; Asher, S. A. *J. Am. Chem. Soc.* **1986**, *108*, 905.
(72) Asher, S. A.; Ludwig, M.; Johnson, C. R. *J. Am. Chem. Soc.* **1986**, *108*, 3186.
(73) Mukherjee, A.; McGlashen, M. L.; Spiro, T. G. *J. Phys. Chem.* **1995**, *99*, 4912.
(74) McGlashen, M. L.; Eads, D. D.; Spiro, T. G.; Whittaker, J. W. *J. Phys. Chem.* **1995**, *99*, 4918.
(75) Shindo, H.; Hiraishi, J. *Chem. Phys. Lett.* **1981**, *80*, 238.
(76) Tripathi, G. N. R.; Schuler, R. M. *Chem. Phys. Lett.* **1982**, *88*, 253.
(77) Kotorlenko, L. A.; Aleksandrova, V. S. *Russ. Chem. Rev.* **1984**, *53*, 1139.
(78) Hockertz, J.; Steenken, S.; Wieghardt, K.; Hildebrandt, P. *J. Am. Chem. Soc.* **1993**, *115*, 11222.
(79) Sokolowski, A.; Müller, J.; Weyhermüller, T.; Schnepf, R.; Hildebrandt, P.; Hildebrandt, K.; Bothe, E.; Wieghardt, K. *J. Am. Chem. Soc.* **1997**, *119*, 8889.
(80) Sokolowski, A.; Leutbecher, T.; Weyhermüller, R.; Schnepf, R.; Bothe, E.; Eckhard, B.; Hildebrandt, K.; Wieghardt, K. *J. Biol. Inorg. Chem.* **1997**, *2*, 444.
(81) Schnepf, R.; Sokolowski, A.; Müller, J.; Bachler, V.; Wieghardt, K.; Hildebrandt, P. *J. Am. Chem. Soc.* **1998**, *120*, 2352.
(82) Berthomieu, C.; Boullais, C.; Neumann, J.-M.; Boussac, A. *Biochim. Biophys. Acta* **1998**, *1365*, 112.
(83) Liu, R.; Zhou, X. *J. Phys. Chem.* **1993**, *97*, 9613.
(84) Liu, R.; Zhou, X. *Chem. Phys. Lett.* **1993**, *207*, 185.
(85) Chipman, D. M.; Liu, R.; Zhou, X.; Pulay, P. *J. Chem. Phys.* **1994**, *100*, 5023.
(86) Yu, H.; Goddard, J. D. *THEOCHEM* **1991**, *233*, 129.
(87) Qin, Y.; Wheeler, R. A. *J. Chem. Phys.* **1995**, *102*, 1689.
(88) O'Malley, P. J. *Chem. Phys. Lett.* **2000**, *325*, 69.
(89) Nwobi, O.; Higgins, J.; Zhou, X.; Liu, R. *Chem. Phys. Lett.* **1997**, *272*, 155.
(90) Guedes, R. C.; Costa Cabral, B. J.; Martinho Simoes, J. A.; Diogo, H. P. *J. Phys. Chem. A* **2000**, *104*, 6062.
(91) Michl, J.; Thulstrup, E. W. *Spectroscopy with Polarized Light. Solute Alignment by Photoselection, in Liquid Crystals, Polymers, and Membranes*; VHS Publishers, Inc.: New York, 1986.
(92) Friderichsen, A. V.; Radziszewski, J. G.; Nimlos, M. R.; Winter, P. R.; Dayton, D. C.; David, D. E.; Ellison, G. B. *J. Am. Chem. Soc.* **2001**, *123*, 1977.
(93) Radziszewski, J. G.; Nimlos, M. R.; Winter, P. R.; Ellison, G. B. *J. Am. Chem. Soc.* **1996**, *118*, 7400. Łapiński, J. G. *Chem. Phys. Lett.* **1999**, *301*, 565.

radicals are all key intermediates in combustion processes, and a knowledge of their spectroscopic fingerprints may lead to a better understanding of the reaction mechanisms and thereby to further progress in the modeling and developing of combustion systems. Our data may also contribute to increasing the information content that can be extracted from diagnostic and analytical measurements of biologically important systems, for example, proteins containing tyrosyl residues. For example, the goal of construction of biomimetic models for galactose oxidase and related enzymes is to model spectroscopic and structural features of the enzymes. In this case, a phenol moiety in tyrosine acts as a built-in cofactor which is oxidized to a substituted phenoxyl radical. This radical then participates in redox reactions catalyzed by the enzyme.[7] We hope that the improved detail of understanding of the vibrational spectrum of the unperturbed phenoxyl radical will contribute to progress in this and other areas of study. The data presented in this paper provide a fingerprint to use in searching for phenoxyl radical in reaction systems and a baseline from which to measure interactions in complex systems that cause shifts in vibrational and electronic absorption bands of the functional phenoxyl radical.

2. Experimental Section

Matrix isolation techniques were applied in the generation and characterization of phenoxyl radicals. The samples were deposited in solid argon in a ratio of 1:1200 at 7−10 K on CsI or CaF_2 spectroscopic windows attached to a coldfinger of the closed-cycle helium refrigerator (APD Cryogenics). The details of sample preparation can be found elsewhere.[92−94] The IR spectra of the matrix samples were recorded with a Magna-560 FTIR instrument (Nicolet) with 0.125 cm^{-1} resolution. The UV−vis spectra were obtained on a Shimadzu 3101 UV−visible−NIR spectrophotometer. The experimental setup enabled recording of electronic and IR spectra on the same sample without moving it. This facility is crucial for obtaining reliable difference spectra and, thus, for unequivocal identification of the species being produced or destroyed.

Phenoxyl radical can be generated from several precursors. It is formed upon irradiation of nitrosobenzene, nitrobenzene, diphenyl peroxide, benzoic anhydride, phenol, anisole, phenetole, or diphenyl carbonate with UV radiation at 248 nm (KrF excimer laser), 254 nm (mercury lamp), 266 nm (Nd:YAG laser, third harmonic), or 308 nm (XeCl excimer laser). In this study, the phenoxyl radicals were prepared from four different precursors: nitrosobenzene (Aldrich, 97%), nitrobenzene (Aldrich, 99%), phenol (Aldrich, 99%), and diphenyl carbonate (Aldrich, 99%). Even though **1** is the major product of the photolysis of the latter two compounds, it is also destroyed at the UV wavelengths most efficiently used for its generation. Therefore, we preferred in most experiments to obtain **1** by photolysis of nitrobenzene or nitrosobenzene using the 308 nm line of an XeCl excimer laser (Lambda Physik Compex-102). Using nitrobenzene leads nearly exclusively to the photoproduction of **1**; minute traces of the phenyl radical are also observed. For the nitrosobenzene precursor, a major product is the phenyl radical. However, **1** is also readily detected: its electronic spectrum dominates that of the phenyl radical because of larger extinction coefficients in the whole visible and UV region. Moreover, **1** can be selectively bleached upon irradiation with visible light (488 or 514 nm). Because phenyl radical is not photochemically destroyed at these wavelengths, its contribution can be subtracted in the difference spectra. In some experiments, polarized light was used for both photogeneration and photodestruction of **1**; subsequent measurements of linear dichroism on the product of precursor photolysis or on a photobleached sample allowed the determination of transition moment directions.

The fully deuterated radical (C_6D_5O, **2**) was produced from perdeuterated nitrobenzene (Aldrich, 99%) or nitrosobenzene (deuterated according to a standard procedure[95]). The singly ^{13}C substituted species (1-$^{13}C^{12}C_6H_5O$, **3**) was obtained by photolysis of phenol-1-^{13}C (Cambridge Isotope Laboratories, 99%).

Table 1. Bond Lengths (Å) and Bond Angles (deg) Predicted for C_{2v} Phenoxyl Radical by UB3LYP/cc-pVTZ

Bond Lengths (Å)	
C1−O	1.2514
C1−C2	1.4486
C2−C3	1.3716
C3−C4	1.4046
C2−H	1.0814
C3−H	1.0822
C4−H	1.0817
Bond Angles (deg)	
C2−C1−O	121.47
C6−C1−C2	117.06
C1−C2−C3	120.85
C2−C3−C4	120.28
C3−C4−C5	120.68
C1−C2−H	117.04
C2−C3−H	120.29
C3−C4−H	119.67

Various approaches have been used to estimate the values of absolute IR intensities. First, they were calculated using the values of the extinction coefficients of the phenoxyl radical in the electronic spectrum.[95] These results could be verified by experiments that monitored the amount of NO that is formed during photolysis of nitrobenzene and the amount of CO arising during photobleaching of **1**. It was assumed that both photoprocesses produce stoichiometric amounts of carbon monoxide and nitric oxide. The absolute IR intensity is known for the former (64 ± 2 km/mol).[96] For the latter, we used the value of 15.3 km/mol, determined for the purpose of this work.

Previous computational investigations have established that an accurate prediction of the molecular structure and vibrations of **1** requires a high level of theory. Two factors were found to be crucial: (i) taking into account the nondynamical electron correlation, and (ii) inclusion of polarization functions into the basis set.[85] In this work, the molecular equilibrium geometry and harmonic force field[97,98] for the phenoxyl radical were computed with the Gaussian98 software package[99] by using UB3LYP[100,101] density functional theory and the cc-pVTZ basis set[102] (280 basis functions, 470 primitive Gaussians). The geometrical parameters predicted for the $^2B_1$ ground-state equilibrium configuration are given in Table 1. Except for a slightly longer C−O distance (0.02 Å), the geometry is very similar to that obtained by the most sophisticated calculations performed so far (CAS-SCF/6-311G(2d,p)).[85] The corresponding electronic energy was −306.939130 Hartree, and the vibrational zero point energy for the parent isotopomer was 0.091414 Hartree (1 Hartree = 4.3597×10^{-18} J). The expectation

(94) Radziszewski, A.; Spanget-Larsen, J.; Langgård, M.; Waluk, J.; Radziszewski, J. G. *J. Phys. Chem.*, in press.

(95) Gorski, A.; Gil, M.; Spanget-Larsen, J.; Waluk, J.; Radziszewski, J. G. *J. Chem. Phys.*, in press.

(96) Radziszewski, J. G.; Hess, B. A., Jr.; Zahradnik, R. *J. Am. Chem. Soc.* **1992**, *114*, 52.

(97) Foresman, J. B.; Frisch, *Æ. Exploring Chemistry with Electronic Structure Methods*; Gaussian, Inc.: Pittsburgh, PA, 1996.

(98) Jensen, F. *Introduction to Computational Chemistry*; Wiley: Chichester, U.K., 1999.

(99) Frisch, M. J.; Trucks, G. W.; Schlegel, H. B.; Scuseria, G. E.; Robb, M. A.; Cheeseman, J. R.; Zakrzewski, V. G.; Montgomery, J. A., Jr.; Stratmann, R. E.; Burant, J. C.; Dapprich, S.; Millam, J. M.; Daniels, A. D.; Kudin, K. N.; Strain, M. C.; Farkas, O.; Tomasi, J.; Barone, V.; Cossi, M.; Cammi, R.; Mennucci, B.; Pomelli, C.; Adamo, C.; Clifford, S.; Ochterski, J.; Petersson, G. A.; Ayala, P. Y.; Cui, Q.; Morokuma, K.; Malick, D. K.; Rabuck, A. D.; Raghavachari, K.; Foresman, J. B.; Cioslowski, J.; Ortiz, J. V.; Stefanov, B. B.; Liu, G.; Liashenko, A.; Piskorz, P.; Komaromi, I.; Gomperts, R.; Martin, R. L.; Fox, D. J.; Keith, T.; Al-Laham, M. A.; Peng, C. Y.; Nanayakkara, A.; Gonzalez, C.; Challacombe, M.; Gill, P. M. W.; Johnson, B. G.; Chen, W.; Wong, M. W.; Andres, J. L.; Head-Gordon, M.; Replogle, E. S.; Pople, J. A. *Gaussian 98*, revision A.3; Gaussian, Inc.: Pittsburgh, PA, 1998.

(100) Becke, A. D. *J. Chem. Phys*. **1993**, *98*, 5648.

(101) Lee, C.; Yang, W.; Parr, R. G. *Phys. Rev. B* **1988**, *37*, 875.

(102) Dunning, T. H., Jr. *J. Chem. Phys.* **1989**, *90*, 1007. Kendall, R. A.; Dunning, T. H., Jr.; Harrison, R. J. *J. Chem. Phys.* **1992**, *96*, 6796. Wilson, A. K.; van Mourik, T.; Dunning, T. H., Jr. *THEOCHEM* **1996**, *388*, 339.

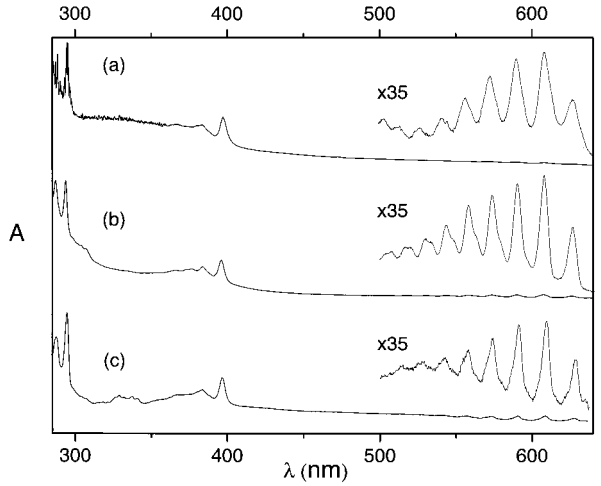

Figure 1. Electronic spectra obtained in Ar matrix at 10 K after (a) irradiation of diphenyl carbonate at 248 nm, (b) irradiation of C_6D_5-NO at 308 nm, and (c) irradiation of 1-^{13}C-phenol at 248 nm.

value of the spin operator S^2 was 0.7864, compared with the value 0.75 for a pure doublet state. IR intensities and Raman scattering activitites for the fundamental vibrational transitions of phenoxyl and its isotopomers were computed by using standard procedures (freq = raman) and default parameters.[99]

3. Results and Discussion

Figure 1 shows the electronic spectra that result during laser photolysis of three different precursors: diphenyl carbonate, deuterated nitrosobenzene, and 1-^{13}C-phenol. The emergence of the absorption bands of **1**[48−56] is observed in all cases. The weak transition in the visible range has its origin around 626 nm. It is followed by two stronger transitions in the UV with origins at about 397 and 294 nm. Even though the electronic spectra of **1**−**3** are very similar, isotopic substitution leads to measurable differences in transition energies. For the low-energy transition, the origins are located at 626.6, 626.1, and 627.6 nm in **1**, **2**, and **3**, respectively. The corresponding values for the second transition are 397.4, 396.2, and 396.8 nm, whereas for the third transition the origins are measured at 295.4, 294.8, and 294.6 nm.

Some features are detected in the electronic spectra that do not belong to the phenoxyl radical. These are the bands lying around 330−340 nm, clearly visible after photolysis of phenol and, with smaller intensity, after photolysis of diphenyl carbonate (cf., Figure 1a,c). We assign these bands to the product of photodestruction of the phenoxyl radical, the cyclopentadienyl radical,[33−38] in accordance with the results obtained in a supersonic jet.[103]

The main reason for using several compounds for generating the phenoxyl radical is to gain access to various IR regions that do not contain the absorption of the precursor. Spectral overlap of the product and precursor bands can thus be avoided, which is particularly advantageous for detection and assignment of weak IR transitions. The choice of the precursor determines the wavelength range for the photolysis. Both nitrobenzene and nitrosobenzene can be transformed into **1** by using 308 nm light. However, the photoreaction paths are very different in the two cases. The photolysis of the former efficiently produces **1**, while, in the case of photolysis of nitrosobenzene, the major product is not **1**, but the phenyl radical.[93] However, the electronic

(103) (a) Sun, S.; Bernstein, E. R. *J. Chem. Phys.* **1995**, *103*, 4447. (b) Applegate, B. E.; Bezant, A. J.; Miller, T. A. *J. Chem. Phys.* **2001**, *114*, 4869.

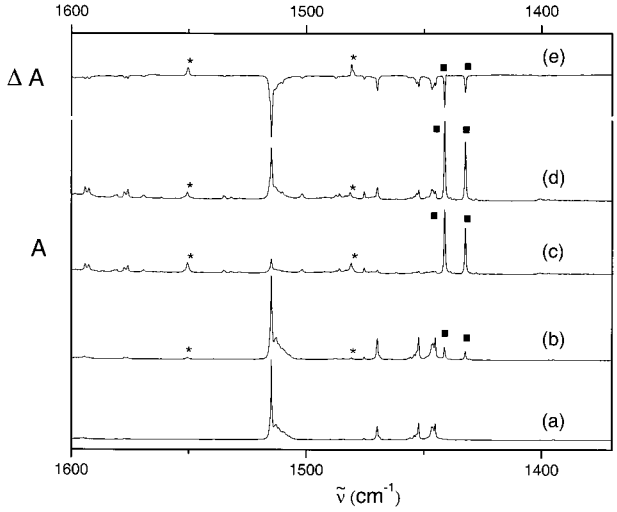

Figure 2. Changes in the IR spectrum accompanying irradiation of nitrosobenzene at 308 nm and subsequent photobleaching of the phenoxyl radical at 488 nm: (a) the spectrum of the precursor; (b), (c) formation of phenyl radical (squares) and phenoxyl radical (stars); (d) the spectrum after bleaching with the 488 nm line; (e), difference between (c) and (d).

spectrum is dominated by the absorption of **1**, because of the much lower values of the extinction coefficients for the only electronic transition of the phenyl radical lying in the range that we use for detection. This transition corresponds to a series of bands starting at about 535 nm, superimposed on the visible absorption of **1** (Figure 1b). The visible transition of **1** is about 30−50 times stronger than that of the phenyl radical.[93−95] We therefore estimate that the quantum yield of photoproduction of **1** is about 10−20 times lower than the yield for the phenyl radical. This could at first disqualify nitrosobenzene as a useful precursor of **1**. However, this is not the case, the reason being that the photolysis of nitrosobenzene can be performed with 308 nm light, whereas the other precursors (except nitrobenzene) require shorter wavelengths, at which the photoproduced **1** is readily destroyed. Thus, a good deal of the results described here for **1** and **2** are based on species produced from nitrosobenzene, for which the destruction of the phenoxyl radical by the photolyzing light could be avoided. The spectral contributions from the phenyl radical could be subtracted by selectively bleaching **1** or **2** with visible lines of the Ar laser. An illustration of this procedure is presented in Figure 2. Irradiation of nitrosobenzene in an Ar matrix with the 308 nm laser line leads to buildup of IR absorptions due to phenyl and phenoxyl radicals and to the decay of the lines due to the precursor (Figure 2b,c). Subsequently, the sample is irradiated with 488 nm photons, leading to a selective depletion of **1** (Figure 2d,e). This can be monitored independently from the electronic absorption spectra that are measured simultaneously with the IR absorption on the same sample. About 65% of **1** disappears after 100 minutes of 488 nm irradiation. Consequently, the lines in the IR spectra whose intensity drops by this amount can be assigned to the phenoxyl radical. The lines due to the phenyl radical[92,94] are only weakly affected; their intensity drops by about 6%. Therefore, they can be subtracted from the spectra, along with the lines due to the nitrosobenzene precursor, which are also not affected by 488 nm irradiation. The IR spectra of **1** and **2** obtained in this way are compared in Figure 3 with the spectra obtained "directly" from photolysis of nitrobenzene. The advantages of using various precursors are evident. For instance, the transition located at 1515 cm^{-1} is clearly seen when **1** is obtained from nitrobenzene (Figure 3b) but not from nitrosoben-

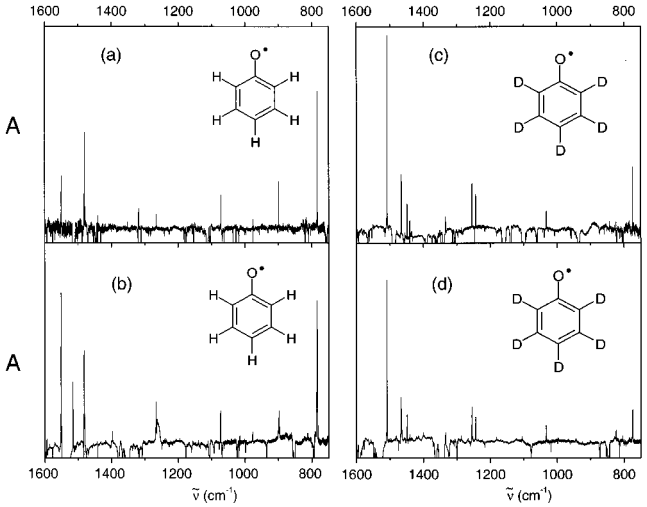

Figure 3. IR spectra of **1** and **2**, obtained after photolysis at 308 nm of nitrosobenzene (a), perdeuterated nitrosobenzene (c), nitrobenzene (b), and perdeuterated nitrobenzene (d). For the nitrobenzene precursors, the spectra shown represent the difference between the absorption curves recorded after and before the 308 nm photolysis. In the case of the nitrosobenzene precursors, the sample was photobleached after the photolysis by using 488 nm radiation: The spectra show the difference between the curves recorded before and after photobleaching.

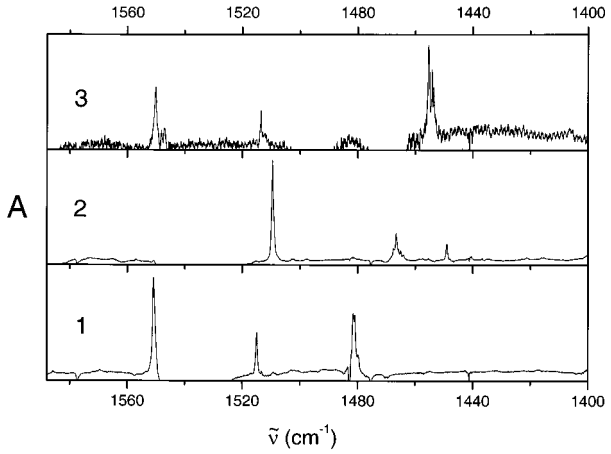

Figure 4. Portions of the IR spectra of **1**−**3**. The spectra of **1** and **2** were obtained from nitrobenzene, while **3** was produced from 1-^{13}C-phenol.

zene (Figure 3a). In the latter case, the 1515 cm^{-1} band is masked by the strong absorption of the precursor. The opposite occurs for the 1318 cm^{-1} band, readily detected during nitrosobenzene photolysis, but difficult to identify when using nitrobenzene as a precursor.

Selective bleaching with visible light has also been used for the sample of **3**, obtained from a different precursor, 1-^{13}C-phenol, by photolysis with 248 nm light. In this case, difference spectra were used to separate lines due to **3** from those due to other possible products of UV photolysis. Figure 4 shows fragments of the IR spectra obtained for **1**−**3** in the "fingerprint" region around 1500 cm^{-1}.

To analyze transition symmetries, linearly polarized UV light was used either in the photolysis or for bleaching of the ensuing photoproducts. In both cases, the resulting, partially oriented sample was investigated by IR linear dichroism (LD) spectroscopy. The LD signal is defined as LD $= E_{\parallel} - E_{\perp}$, the difference between the absorbances measured with the electric vector of light parallel ($E_{\parallel}$) and perpendicular ($E_{\perp}$) to the electric vector of the light used for photolysis or photobleaching. The sign of

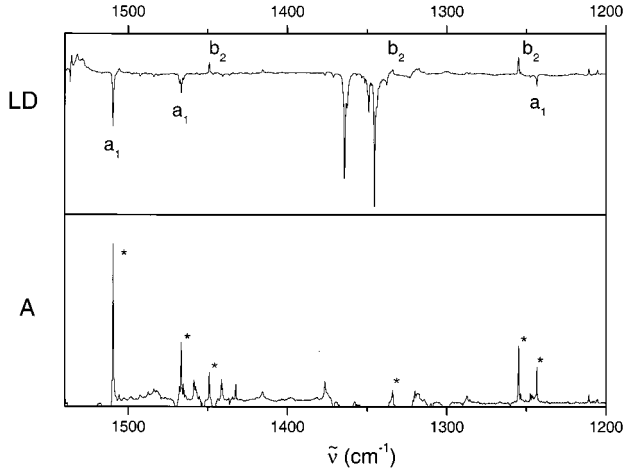

Figure 5. Portion of the absorption and LD IR spectra obtained after photobleaching of **2** with polarized UV radiation at 248 nm. The peaks due to **2** are indicated by asterisks; the remaining peaks are mainly due to the precursor (perdeuterated nitrobenzene).

the LD signal observed for a vibrational transition depends on the orientation of the moment direction for this transition relative to that of the electronic transition involved in the photolysis or photobleaching experiment.

In the case of the photobleaching experiment, the analysis is relatively straightforward, and it is further simplified by the C_{2v} molecular symmetry of **1**. If the electronic transition active in the bleaching process is polarized along the C_2 molecular axis (z), the surviving phenoxyl radicals will have their molecular C_2 axes oriented preferentially perpendicular to the electric vector of the bleaching light. Therefore, the LD should be negative for z-polarized vibrational transitions (a_1 symmetry species) and positive for y- and x-polarized transitions (b_1 and b_2 species). This is illustrated in Figure 5, which shows part of the LD IR spectrum measured after photobleaching of **2** with polarized light of 248 nm wavelength: a_1 vibrations exhibit negative LD, and b_2 vibrations positive LD.

The situation is different in the case when the partially oriented sample of **1** is obtained as a result of photolysis with linearly polarized light. If the electronic transition active in the photoreaction is polarized close to the "long axis" of the precursor (and the photoreaction does not involve significant rotation of the reactants), the IR LD would be expected to be positive for a_1 vibrations and negative for b_1 and b_2 vibrations. Our IR LD experiments performed for **1** obtained from nitrobenzene as a precursor revealed negative LD for a_1 vibrations. This would indicate "short axis" polarization of the precursor transition, in nice agreement with recent results obtained for gas-phase nitrobenzene molecules oriented in an electric field.[104]

The analysis of the spectra was supported by the results of quantum chemical calculations. Tables 2−4 compare the experimentally determined and calculated fundamental vibrational transitions. Strong arguments for the assignments were provided by a consideration of the isotopic wavenumber shifts, because these are usually more easily predicted by quantum chemical procedures than the absolute wavenumbers of the transitions.

Among the 30 fundamental vibrations of **1**, 27 are IR-active ($11a_1 + 6b_1 + 10b_2$). In the following, we discuss the results and assignments in detail, comparing the experimental data with

(104) Castle, K. J.; Abbot, J.; Peng, X.; Kong, W. *J. Chem. Phys.* **2000**, *113*, 1415.

Table 2. Vibrations of Phenoxyl Radical, C_6H_5O (**1**)

		exptl[a]			calcd[b]			
	sym	$\tilde{\nu}$	I	$\tilde{\nu}$ (RR)	$\tilde{\nu}$	I	*A*	assignment[c]
1	a_1	3090	<0.4		3199	1.2	330.7	CH str (20a)
2		3065	3.7		3188	13.6	64.7	CH str (13)
3		3018	<0.4		3166	0.8	39.3	CH str (2)
4		1550	36.8	1552[d]	1589	38.0	41.4	CC str (8a)
5		1481	31.0	1502[d]	1482	20.9	54.1	CO str (7a)
6		1397	1.8	1398[e,f]	1422	0.2	8.0	CH bend/CC str (19a)
7		1167	1.5	1157[e]	1167	0.3	13.5	CH bend (9a)
8		1038	0.1	1050[g]	1011	0.1	26.1	CH bend/ring breath (12)
9		977	3.2	990[d,e]	991	2.4	2.5	CCC bend (18a)
10		813	1.1	801[d]	807	1.6	14.5	ring breath/CCC bend (1)
11		520	2.9	528[e]	533	2.3	8.0	CCC bend (6a)
12	a_2				996	0.0	0.1	HCCH tor (17a)
13					809	0.0	0.9	CH wag (10a)
14					383	0.0	0.0	ring def (16a)
15	b_1	1016	0.6		1010	0.2	0.0	HCCH tor (5)
16		898	14.0		936	8.8	0.0	CH wag/boat def (17b)
17		784	42.1		808	37.2	0.2	chair def/CO CH wag (4)
18		635	58.4		660	40.6	0.2	chair def/CH wag (11)
19		472	0.6		487	0.8	0.0	boat def/CO wag (16b)
20					191	2.5	1.3	boat def/CO wag (10b)
21	b_2	3074	4.8		3196	8.2	15.0	CH str (20b)
22		3054	<0.5		3172	8.5	122.4	CH str (7b)
23		1515	9.6		1550	4.5	1.8	CC str/CH bend (~19b)
24		1441	0.2		1449	3.2	2.6	CH bend/CC str (~8b)
25		1318	7.8	1331[e]	1340	6.2	0.8	CC str/CH bend (14)
26		1266	8.8		1277	6.4	1.9	CC str/CH bend (3)
27		1140	1.3		1167	1.4	1.4	CH bend/CC str (15)
28		1072	10.5		1092	8.6	2.2	CH bend/CC str (~9b)
29		616	2.0		599	0.5	5.9	CCC bend (6b)
30		446	6.4		447	4.6	0.2	CO bend (~18b)

[a] Argon matrix; $\tilde{\nu}$, in cm^{-1}; *I*, absolute intensity in km/mol; estimated accuracy, ±30%; RR, resonance Raman measurements. [b] B3LYP/cc-pVTZ. No scaling; *A*, Raman scattering activity in $Å^4$/amu. [c] Approximate mode description, Wilson's notation in parentheses. [d] Ref 71. [e] Ref 66. [f] Ref 73. [g] Ref 67.

the theoretical predictions and with results of previous Raman measurements. While making assignments, we often refer to Wilson's nomenclature,[105,106] being aware of its ambiguities, but keeping it to facilitate comparison with previous experimental and theoretical studies.

3.1 a_1 Vibrations. CH Stretching Region. Three moderately intense bands that reveal LD signs corresponding to a_1 symmetry are observed at 3065, 2949, and 2868 cm^{-1}. The wavenumber of the highest energy transition is in perfect agreement with the prediction obtained by an RR-based force field (3067 cm^{-1}).[73] The other two bands are located at wavenumbers too low to be assigned to the CH stretches. The spread of these three frequencies over nearly 200 cm^{-1} would be rather unusual; the calculations predict them to be contained within 33 cm^{-1} in **1** and within 36 cm^{-1} in **2**. This prediction is almost fulfilled for **2** where the experimental wavenumbers are 2331, 2298, and 2284 cm^{-1}; in this case, the assignment to CD stretches appears safe. In the case of **1**, we assign the 3065 cm^{-1} transition to a CH stretching fundamental, the 2949 cm^{-1} band to an overtone ($2 \times 1481 - 13$), and the 2866 cm^{-1} band to a combination level ($1481 + 1397 - 12$). Several low intensity bands detected in the 3010−3090 cm^{-1} region are good candidates for the remaining CH stretching vibrations. However, because of mutual overlap and overlap with bands due to precursors and other photolysis products (phenyl radical), the assignments for the two weak bands are extremely difficult and should be treated as tentative. As predicted by theory, one a_1 CH fundamental is much stronger than the other two, and only this can be safely assigned (3065 cm^{-1}).

1550 cm^{-1}. A very strong transition is observed for **1** at 1550 cm^{-1}. It shifts by 41 cm^{-1} in **2** and remains at the same position in **3**. A safe assignment is to the CC ring stretch (ν_{8a} in Wilson's notation), calculated at 1589 cm^{-1}; the computed isotope shifts for **2** and **3** are 44 and 0 cm^{-1}, respectively. This transition has been observed by RR at 1557,[73] 1552,[71] and 1558 cm^{-1}.[64] Characteristically, it was resonance-enhanced for excitations at 240,[73] 245,[71] and 416 nm,[64] but not at 400 nm.[66] It should be noted that these four wavelengths correspond to transitions to three different electronic states of the phenoxyl radical. In particular, 400 and 416 nm excitations correspond to different $\pi\pi^*$ electronic levels, presumably $^2B_1$, and $^2A_2$.[95] For the latter electronic state, theoretical considerations[85] predicted resonance Raman enhancement of the ν_{8a} mode, while, for the former, the enhancement of the CO stretch (ν_{7a}) mode was predicted. Being perfectly consistent with previous Raman and our present IR measurements, these predictions also provide strong support for the symmetry assignments of the two electronic states.

1481 cm^{-1}. The strongest Raman band of **1**, assigned to the CO stretching mode (ν_{7a}), has been reported at 1505,[66,73] 1502,[71] and 1518 cm^{-1}.[64] We assign the intense IR band observed at 1481 cm^{-1} and calculated at 1482 cm^{-1} to this fundamental. The difference between the Raman frequency obtained in alkaline aqueous solutions and the IR frequency for a matrix-isolated molecule is quite substantial. However, it is not unexpected. As indicated by the absolute value of the CO stretch frequency, which is much larger than that in phenol (1255 cm^{-1}),[107] the carbon−oxygen bond in **1** has considerable double bond character, corresponding to a quinoid contribution. This contribution may vary with solvent polarity, being larger in a polar environment, where the frequency should be correspondingly higher. Large differences were observed by RR for two combination bands of **1** upon changing solvent from water to ethanol or carbon tetrachloride: red shifts of 22 and 28 cm^{-1} were measured for CCl_4.[64] An additional effect may be due to specific interactions of the CO group with water and, in particular, metal ions present in the alkaline solutions. Theoretical simulations[88] predict that the phenoxyl radical exists as an ion complex under these conditions; a large blue shift of 69 cm^{-1} was calculated for the complexed form. It is likely that both specific and nonspecific effects add up to produce differences in CO stretching frequencies in different environments.

The shifts observed in the matrix for the 1481 cm^{-1} band of **1** are 14 and 26 cm^{-1} for **2** and **3**, respectively. The same shift was observed upon $h_5 \rightarrow d_5$ substitution for the 1505 cm^{-1} Raman band,[66,73] which assures us of the assignment. Interestingly, both the present and nearly all previous theoretical results predict an isotopic shift on perdeuteration that is about twice too large.[85] On the other hand, the calculations underestimate the shift upon 1-^{13}C substitution. We have presently no obvious explanation for these discrepancies, but possibly interaction with the matrix is significant for the CO stretching mode.

(105) Wilson, E. B. *Phys. Rev.* **1934**, *45*, 706.
(106) Stephenson, C. V.; Coburn, W. C., Jr.; Wilcox, W. S. *Spectrochim. Acta* **1961**, *17*, 933.
(107) Tripathi, G. N. R. *J. Chem. Phys.* **1979**, *71*, 4025.

Table 3. Vibrations of C_6D_5O (**2**)

	exptl[a]				calcd[b]				
ν	sym	$\tilde{\nu}$	I	Δ	$\tilde{\nu}$ (RR)[d]	$\tilde{\nu}$	I	Δ	A	assignment[c]
1	a_1	2331	0.3			2371	0.7	828	150.9	CH str (20a)
2		2298	1.7	766		2355	12.0	833	16.4	CH str (13)
3		2284	0.3			2335	0.2	831	13.3	CH str (2)
4		1509	41.8	41		1545	36.6	44	42.0	CC str (8a)
5		1467	22.6	14	1489	1445	10.5	37	68.2	CO str (7a)
6		1244	5.7	153	1234	1268	3.6	154	8.1	CH bend/CC str (19a)
7		844	0.7	323	846	844	0.4	323	11.2	CH bend (9a)
8		902	0.6	136		869	0.0	142	23.1	CH bend/ring breath (12)
9		944	1.7	33		962	2.4	29	6.3	CCC bend (18a)
10		724	1.4	89	732	733	1.7	74	5.4	ring breath/CCC bend (1)
11		505	2.8	15	514	518	2.3	15	6.8	CCC bend (6a)
12	a_2					802	0.0	194	0.1	HCCH tor (17a)
13						629	0.0	180	0.0	CH wag (10a)
14						336	0.0	47	0.0	ring def (16a)
15	b_1	860	3.3	156		855	2.5	155	0.2	HCCH tor (5)
16		775	11.3	123		799	9.0	137	0.2	CH wag/boat def (17b)
17		660	18.0	124		678	6.3	130	0.1	chair def/CO CH wag (4)
18		489	31.1	147		508	27.6	152	0.2	chair def/CH wag (11)
19		406	1.8	66		421	2.8	66	0.0	boat def/CO wag (16b)
20						179	2.7	12	0.7	boat def/CO wag (10b)
21	b_2	2326	0.7	748		2366	6.9	830	1.4	CH str (20b)
22		2281	0.4	773		2341	3.5	831	62.8	CH str (7b)
23		1449	4.7	66		1473	1.4	77	1.4	CC str/CH bend (~19b)
24		1334	4.2	107	1369	1360	7.3	89	3.0	CH bend/CC str (~8b)
25		1255	9.7	63		1273	11.0	67	0.3	CC str/CH bend (14)
26		1032	2.5	234		1051	1.4	226	0.2	CC str/CH bend (3)
27		836	2.8	304		855	1.8	312	3.9	CH bend/CC str (15)
28		824	3.0	268		824	2.3	268	0.3	CH bend/CC str (~9b)
29						578	0.4	21	5.6	CCC bend (6b)
30		423	2.8	23		425	4.7	22	0.3	CO bend (~18b)

[a] Argon matrix; $\tilde{\nu}$, in cm^{-1}; I, absolute intensity in km/mol; estimated accuracy, ±30%; Δ [cm^{-1}], observed and calculated isotopic shifts with respect to **1**. [b] B3LYP/cc-pVTZ. No scaling; A, Raman scattering activity in $Å^4$/amu. [c] Approximate mode description. [d] Ref 66.

Table 4. Fundamental Vibrations of 1-^{13}C Labeled Phenoxyl, 1-$^{13}C^{12}C_5H_5O$ (**3**)

	exptl[a]				calcd[b]				
ν	sym	$\tilde{\nu}$	I	Δ	$\tilde{\nu}$	I	Δ	A	assignment[c]
1	a_1				3199	1.2	0	330.7	CH str (20a)
2		3066	3.8	−1	3188	13.6	0	64.6	CH str (13)
3					3166	0.8	0	39.3	CH str (2)
4		1550	20.7	0	1588	36.4	1	40.2	CC str (8a)
5		1455	38.3	26	1465	19.0	17	38.3	CO str (7a)
6		1381	1.3	16	1405	3.4	17	22.8	CH bend/CC str (19a)
7					1167	0.3	0	14.5	CH bend (9a)
8					1011	0.1	0	26.2	CH bend/ring breath (12)
9		976	5.8	1	991	2.5	0	2.5	CCC bend (18a)
10		810	3.1	3	804	1.4	3	13.9	ring breath/CCC bend (1)
11					529	2.3	4	7.7	CCC bend (6a)
12	a_2				996	0.0	0	0.1	HCCH tor (17a)
13					809	0.0	0	0.9	CH wag (10a)
14					383	0.0	0	0.0	ring def (16a)
15	b_1				1010	0.2	0	0.0	HCCH tor (5)
16		895	4.2	3	933	7.7	3	0.0	CH wag/boat def (17b)
17		774	76.7	10	798	41.4	10	0.2	chair def/CO CH wag (4)
18		632	76.7	3	657	37.5	3	0.2	chair def/ CH wag (11)
19					482	0.8	5	0.1	boat def/CO wag (16b)
20					191	2.5	0	1.3	boat def/CO wag (10b)
21	b_2	3071	>1.9	3	3196	8.2	0	15.0	CH str (20b)
22				0	3172	8.5	0	122.4	CH str (7b)
23		1513	10.3	2	1548	4.4	2	1.7	CC str/CH bend (~19b)
24		1435	0.8	6	1443	3.9	6	3.0	CH bend/CC str (~8b)
25		1318	4.6	0	1340	6.1	0	0.8	CC str/CH bend (14)
26		1242	1.2	24	1253	5.2	24	1.5	CC str/CH bend (3)
27					1167	1.3	0	1.5	CH bend/CC str (15)
28		1070	>0.8	2	1090	9.0	2	2.1	CH bend/CC str (~9b)
29					598	0.5	1	5.9	CCC bend (6b)
30					445	4.6	2	0.2	CO bend (~18b)

[a] Argon matrix; $\tilde{\nu}$, in cm^{-1}; I, absolute intensity in km/mol; Δ [cm^{-1}], observed and calculated isotopic shifts with respect to **1**. [b] B3LYP/cc-pVTZ. No scaling; A, Raman scattering activity in $Å^4$/amu. [c] Approximate mode description.

1397 cm^{-1}. This weak band has also been detected by RR spectroscopy.[66,71,73] It was initially assigned to a nontotally symmetric vibration,[66,71] but recent work favors the assignment to an a_1 species (CC stretch, ν_{19a}).[67,73] Our data agree with the latter conclusion. In **2**, we find this vibration at 1244 cm^{-1}. The observed and calculated shifts are in perfect agreement (153 and 154 cm^{-1}, respectively). It should also be noted that the theory correctly predicts the increase in intensity of this band upon deuteration.

1167 cm^{-1}. We assign this transition to the CH bending vibration (ν_{9a}), calculated at 1167 cm^{-1}, in agreement with previous Raman results for the band observed at 1164,[71] 1163,[73] and 1157 cm^{-1}.[66] The corresponding band in **2** is found at 844 cm^{-1}, in exact agreement with the calculated value. In the RR studies of **2**,[66] the authors assigned the frequency at 846 cm^{-1} to the CH bending (ν_{18a}) mode, while the frequency detected at 865 cm^{-1} was assigned to ν_{9a}. They noted, however, that the assignments of the "9a and 18a modes may possibly be interchanged".

1038 cm^{-1}. This weak IR band corresponds to the 1050 cm^{-1} vibration observed by RR and assigned to a mixture of Wilson modes 1 and 12 (ring breath/CCC bend).[67] We would rather describe the nuclear motions as CH bend/ring breath (ν_{12}). The observed shift in the fully deuterated species is 136 cm^{-1}; the calculations give 142 cm^{-1}.

977 cm^{-1}. We assign this band to the CCC bend (ν_{18a}) calculated at 991 cm^{-1}. It corresponds to a Raman transition detected at 990[66,71] and 1004 cm^{-1}.[64] The predicted shifts are 29 and 0 cm^{-1} for **2** and **3**, in nice agreement with the experimental values of 33 and 1 cm^{-1}, respectively. As mentioned above, it was previously proposed that either the 865 or the 846 cm^{-1} RR band observed for **2** might correspond to this mode. We are in favor of the present assignment which leads to excellent consistency between experiment and theory.

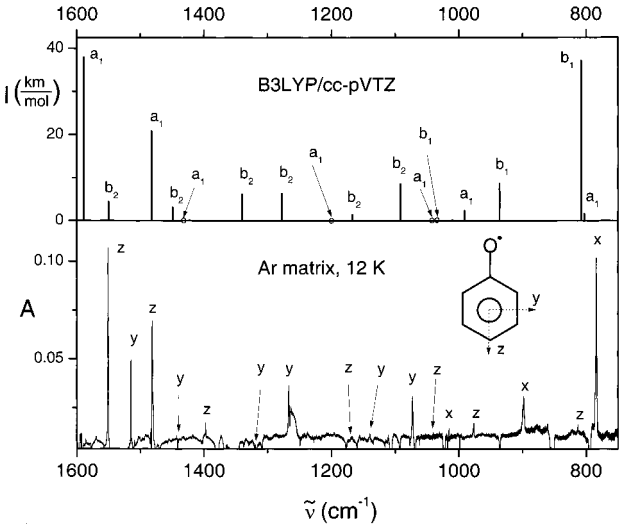

Figure 6. Theoretical (top) and experimentally determined (bottom) IR frequencies for the phenoxyl radical (**1**).

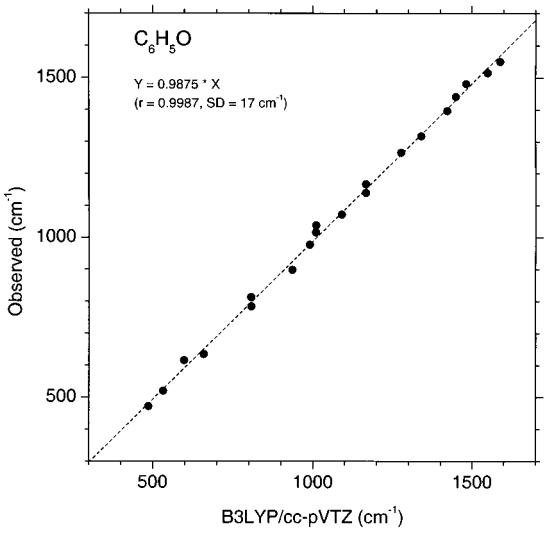

Figure 7. Correlation of observed and calculated vibrational wavenumbers for the phenoxyl radical (**1**).

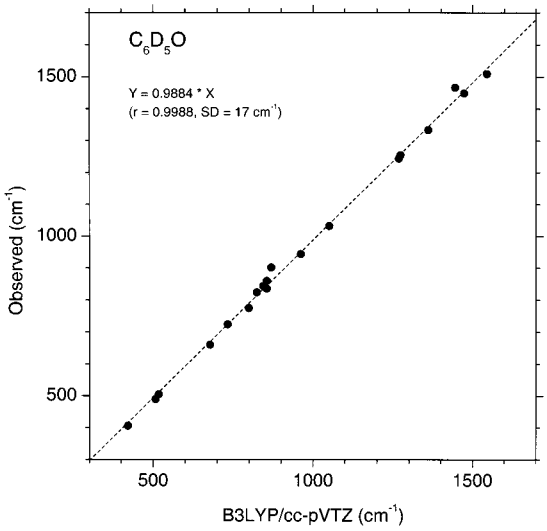

Figure 8. Correlation of observed and calculated vibrational wavenumbers for the perdeuterated phenoxyl radical (**2**).

813 cm^{-1}. A corresponding Raman transition was observed at 801 cm^{-1} [71] and assigned to ring breath/CCC bend (ν_1), in accordance with our present findings. The observed shifts in **2** and **3** are 89 and 3 cm^{-1}; the calculated ones are 74 and 3 cm^{-1}.

520 cm^{-1}. This vibration corresponds to a CCC bending vibration (ν_{6a}), detected previously by Raman spectroscopy at 528 cm^{-1}.[67] Our data for **2** yield a 15 cm^{-1} isotope shift, exactly as predicted by our calculations.

3.2 b_1 Vibrations. No vibrations of this symmetry species have been reported so far. The B3LYP/cc-pVTZ calculations predict weak Raman, but strong IR, intensities. Indeed, the predicted IR transitions are readily observed.

1016 cm^{-1}. This vibration corresponds to the HCCH torsion (ν_5), predicted to shift by 155 cm^{-1} upon deuteration, in agreement with the experimental value of 156 cm^{-1}.

898 cm^{-1}. This moderately intense band corresponds to a vibration described by CH wag/boat deformation (ν_{17b}). The frequency shift upon $h_5 \rightarrow d_5$ substitution, 123 cm^{-1}, correlates well with the theoretical value of 137 cm^{-1}. The experimental and theoretical values for 1-^{13}C substitution shift are the same, 3 cm^{-1}.

784 cm^{-1}. A very strong band that shifts in **3** by 10 cm^{-1}, exactly as predicted by theory, can be safely assigned to a chair deformation/CO,CH wagging mode (ν_4). For **2**, the experimental and theoretical shifts are 124 and 130 cm^{-1}, respectively.

635 cm^{-1}. This is another strong transition, assigned to a combination of chair deformation/CH wagging motions (ν_{11}). The shift in **2** is 147 cm^{-1}, to be compared with the theoretical value of 152 cm^{-1}. Both experiment and theory yield the same value of shift in **3**, 3 cm^{-1}.

472 cm^{-1}. This is a weak band, assigned to a combination of boat deformation/CO wag (ν_{16b}), shifted by 65 cm^{-1} in **2** (the theoretical value is 66 cm^{-1}).

3.3 b_2 Vibrations. The only modes of this symmetry mentioned in the literature for **1** correspond to a weak RR band at 1331 cm^{-1} [66] and to a band at 1398 cm^{-1}.[66,71] The latter, however, as already discussed, should rather be assigned to a totally symmetric vibration. For the former, we find a corresponding IR transition of this symmetry, along with all other b_2 modes.

CH stretches. In **2**, the bands observed at 2326 and 2281 cm^{-1} can safely be assigned to CD stretches. In **1** and **3**, the situation is more complicated, for the same reasons as described above for the corresponding a_1 vibrations. We tentatively assign the bands observed at 3074 and 3054 cm^{-1} for **1** to CH stretches.

1515 cm^{-1}. This band, assigned to a combination of CC stretch and CH bend (ν_{19b}), is shifted to 1449 cm^{-1} for **2** and 1513 cm^{-1} for **3**. The experimental shifts of 66 and 2 cm^{-1} compare favorably with the theoretical values of 77 and 2 cm^{-1}.

1441 cm^{-1}. Again, this transition may be assigned to a combination of CH bend and CC stretch (ν_{8b}), calculated at 1449 cm^{-1}. The corresponding bands are located at 1334 cm^{-1} in **2**, and at 1435 cm^{-1} in **3**.

1318 cm^{-1}. As predicted by theory, the position of this band, which we assign to a combination of CC stretch and CH bend (ν_{14}), remains the same in **1** and **3**. In **2**, it is shifted by 63 cm^{-1}, to be compared with a prediction of 67 cm^{-1}. Most probably, this vibration corresponds to a Raman band observed at 1331 cm^{-1},[66] although the reported shift upon deuteration, 97 cm^{-1}, is significantly higher than in our experiment and difficult to explain.

1266 cm^{-1}. This band is another combination of CC stretching and CH bending motions (ν_3). The corresponding band in **2** is predicted to be very strongly shifted, by 226 cm^{-1}. Experimentally, we find a value of 234 cm^{-1}. The calculated shift for **3** is 24 cm^{-1}, in exact agreement with experiment if

the weak band observed at 1242 cm^{-1} is assigned to this mode. While highly probable, the experimental assignment is less certain in this case, because the band at 1242 cm^{-1} strongly overlaps with the absorption of the precursor of **3**, 1-^{13}C-phenol.

1140 cm^{-1}. An extremely weak transition is observed at this frequency for **1**. It exhibits the LD sign appropriate for b_2 symmetry. We tentatively assign it to the ν_{15} mode calculated at 1167 cm^{-1}. The corresponding band in **2** is expected to be located around 828 cm^{-1}. We observe transitions at 824 and 836 cm^{-1} and assign the latter to ν_{15}, and the former to another vibration of b_2 species, as discussed below.

1072 cm^{-1}. The assignment of this moderately intense band to a CH bend/CC stretch combination (ν_{9b}) seems safe, even though for **3** this band overlaps with strong absorption due to the precursor. The predicted $h_5 \rightarrow d_5$ isotope shift of 268 cm^{-1} suggests the location of the corresponding band in **2** at 824 cm^{-1}, exactly where we observe an IR transition.

616 cm^{-1}. This band is assigned to a CCC bend vibration (ν_{6b}), expected to shift by 21 cm^{-1} in **2**. We do observe an extremely weak transition in **2** at 591 cm^{-1}. However, the intensity is too low for a reliable assignment.

446 cm^{-1}. This is a CO bending vibration, predicted to shift in **2** by 22 cm^{-1} (23 cm^{-1} is observed).

4. Conclusions

This investigation has led to detection and assignment of all but one IR-active fundamental vibrational modes of the phenoxyl radical, most of which have not been observed previously. The only remaining fundamental should be located below 200 cm^{-1}, outside the limits of our detection range. The vibrational assignments were based on the results of linear dichroism measurements and on the analysis of observed and calculated isotope shifts. The agreement between experimental and theoretical IR transitions is highly satisfactory. Evidently, computational chemistry has reached a level that makes it an extremely valuable and reliable tool for the study of molecular and vibrational structure of moderately sized molecules, even in the case of radicals. Comparison of experimental and theoretical IR spectra for **1** is presented in Figure 6, while Figures 7 and 8 show the scaling regressions of observed and calculated wavenumbers for **1** and **2**. The standard deviations, 17 cm^{-1} in both cases, may be compared with the corresponding values of 14 and 12 cm^{-1} previously obtained for the phenyl radical and its perdeuterated isotopomer.[94]

The vibrational wavenumbers reported in this work, measured in inert matrices, are probably much closer to the values expected for an isolated gas phase molecule than those previously reported on the basis of Raman measurements in polar environments. Quite substantial differences are observed between the two data sets. In particular, the frequency of the CO stretching vibration is much lower in matrix-isolated samples (21 cm^{-1} in **1**, 23 cm^{-1} in **2**). As discussed above, this finding demonstrates an increased degree of quinoid character of **1** in polar and protic solvents. The strong sensitivity of the CO stretching wavenumber to environmental effects such as solvent polarity and complex formation makes this mode particularly useful for structural and analytical applications.

We hope that our work can contribute to a better understanding of the structure of the phenoxyl radical, provide new means for its spectral detection and monitoring, and stimulate further theoretical work. The experimental methods applied in this investigation are not limited to IR measurements. In a separate paper,[95] we apply polarization spectroscopy in a discussion of the nature of the electronic transitions of **1**.

Acknowledgment. J.G.R. is grateful for generous financial support from the NREL FIRST and DDRD programs. Morten Langgård of H. Lundbeck A/S is acknowledged for help with the calculations. The experimental work was supported in part by DURIP Grant F49620-99-1-0150 and funds from CSM. Encouragement and support by Dr. Gene Peterson (NREL) is also acknowledged.

JA0113596